

Monte Carlo analysis of earthquake resistant R-C 3D shear wall-frame structures

Beyza Taskin[†] and Zeki Hasgür[‡]

Istanbul Technical University, Department of Civil Engineering, Maslak, Istanbul, Turkey

(Received December 4, 2003, Accepted November 3, 2005)

Abstract. The theoretical background and capabilities of the developed program, SAR-CWF, for stochastic analysis of 3D reinforced-concrete shear wall-frame structures subject to seismic excitations is presented. Incremental stiffness and strength properties of system members are modeled by extended Roufaiel-Meyer hysteretic relation for bending while shear deformations for walls by Origin-Oriented hysteretic model. For the critical height of shear-walls, division to sub-elements is performed. Different yield capacities with respect to positive and negative bending, finite extensions of plastic hinges and P - δ effects are considered while strength deterioration is controlled by accumulated hysteretic energy. Simulated strong motions are obtained from a Gaussian white-noise filtered through Kanai-Tajimi filter. Dynamic equations of motion for the system are formed according to constitutive and compatibility relations and then inserted into equivalent Itô-Stratonovich stochastic differential equations. A system reduction scheme based on the series expansion of eigen-modes of the undamaged structure is implemented. Time histories of seismic response statistics are obtained by utilizing the computer programs developed for different types of structures.

Key words: non-linear analysis; stochastic; white-noise, shear wall-frame systems; reinforced concrete; Monte-Carlo simulation.

1. Introduction

The aftermath of recent destructive great Kocaeli, August 1999 ($M_s = 7.4$) and November 1999 Düzce ($M_s = 7.2$) earthquakes in Turkey have demonstrated the need for reliable evaluation of structural safety against severe random load reversals. This is particularly true for medium to high-rise reinforced concrete (RC) buildings where components are stressed beyond their elastic limits.

On the other hand, as described in Mochizuki and Goto (1983), the distribution of the ultimate shear strength coefficients of RC framed structural systems in some cases had placed in a very narrow range of S_{BG} indices of 0.25~0.37 due to the paucity of total amount of columns and effective walls. Meanwhile, after high casualties and damage, it is again convinced that besides the irregular bearing system and low material strength, the lack of shear walls was one of the essential problems (Aydan *et al.* 1999). For retrofitting purposes, it is necessary to supplement the present, slight to moderate damaged RC frame system with the effective classical shear wall and column jacketing techniques in highly seismic regions. The aseismic design practice relies on hysteretic

[†] Assistant Professor, Corresponding author, E-mail: btaskin@ins.itu.edu.tr

[‡] Professor

energy dissipation of the structural components, including shear walls, through inelastic cyclic deformations while the presence of shear walls have significant importance in earthquake resistance (Hasgür *et al.* 2003). Under the effect of dynamic earthquake loads, the behaviors of the elements consisting a shear wall-frame system vary in time with respect to their deformations. In other words, the force-deformation or moment-curvature relations vary in a non-linear character. Recently, considering the deterministic analyses, hysteretic models are observed to be classified into two groups: The first group, which is more concentrated on global modeling, therefore, preferring simpler models, try to implement many degrading characteristics by rather simpler parameters substituted into the former models as in Umemura *et al.* (2001) and Leztuzzi and Badoux (2003). The second group mostly concerns the members' structural characteristics, considering confinement ratio, plastic hinge formation depending flexural or shear failure, as in Saatçioğlu and Özcebe (1989), D'Ambrisi and Filippou (1999) and ElMandooh Galal and Ghobarah (2003) which are pronounced here as their significance among the huge research done in the area.

Due to the random nature of earthquake strong motions and random characteristics of responses, analytical solutions for mean values and covariances of story displacement or end-section moments can be obtained, using equivalent linearization or equivalent polynomial expansion techniques for the stochastic analysis of plane frames (Nielsen *et al.* 1989). However, accurate analytical solutions, for the stochastic response of the state variables controlling the damage of the structures had turned out to be more difficult to obtain (Mørk 1989). An alternative approach is based on Monte-Carlo (MC) simulation. In this simulation technique, depending on sufficiently stabilized estimates of mean values and covariances, the number of independent samples needed increases dramatically as the computational effort increases sharply. Pradlwarter and Schuëller (1999), discussed various procedures to extent the applicability and the efficiency of MC simulation for the analysis of complex dynamical systems. In particular, the capabilities of the methods denoted Russian Roulette and Splitting (RR&S) or Double and Clump (D&C) are reviewed with the aspect of analyzing such systems. In their later studies, Enam *et al.* (2000) proposed a procedure, which combines the finite element analysis with statistical linearization to reduce the computational efforts required, when compared to direct MC simulation.

The modeling of the restoring force and response analysis of the inelastic structure under random excitations is somewhat a difficult problem although researches on random vibration of structures and structural systems have made great progress. An overview of the major developments in the modeling and response analysis of inelastic structures subjected to random vibrations is summarized in Wen (1989). Recent developments include: (1) a method of modeling hereditary behavior of inelastic systems under biaxial and uniaxial loads; (2) methods of solution including those based on semiempirical approaches, the Fokker-Planck equation and equivalent linearization; and (3) applications for performance and safety evaluation of actual structural systems. Exact modeling of the interaction of bending moments and axial force in the constitutive relations of section requires at least a two-dimensional incremental flow rule. Since, this increases the computational efforts dramatically, Roufaiel and Meyer (1987) suggested a simplified model where the initial moment capacity is increased in proportion to the compression force in the statical equilibrium state.

Early models, for response analysis of RC beam elements assumed zero length of plastic end zones (Clough and Johnston 1966, Giberson 1969, Otani and Sözen 1972). Such one-dimensional hinge models usually lead to conservative estimates of rotational ductility capacity of the end sections. Ones that are more complicated e.g., Takeda (1970), Bouc (1971), Baber and Wen (1979) follow these mostly bilinear models, introducing degrading characteristics such as strength

degradation, strain hardening, stiffness degradation effects associated with unloading and load reversal stages or shear effects by either multi-linear or smooth skeleton curves. The question whether deformation capacity should be measured in terms of inelastic curvature or inelastic rotations is entirely discussed an extensive collection of rotation capacity data is reported by Casciati and Favre (1989), which includes 310 tests performed in sixteen different laboratories in twelve countries. Meanwhile, in order to consider the effect of cumulative seismic damage, Shinozuka, Wen and Casciati (1990) presented automated damage-control design procedure in the modified form of Miner's rule for RC frames.

A number of computer programs for deterministic seismic analysis of plane reinforced concrete buildings subjected to predefined earthquake accelerations have been published in the past. The program SAKE (Otani 1974) based on the Otani-Sözen model is capable of modelling symmetric cross section for framed structures. LARZ (Lopez 1988) based on Takeda and origin-oriented hysteretic models should be mentioned for the RC plane frame-wall structures. Unsymmetrical sections are considered by the programs SARCF-II (Rodriguez-Gomez *et al.* 1990) that is based on the model by Roufaiel & Meyer, DRAIN-2DX (Prakash *et al.* 1993) and IDARC 2D (Park *et al.* 1996) handling plane-frame problems. A few software on the topic dealing with 3D problems are published among which DRAIN-3DX (Prakash *et al.* 1994) has significant importance. Certainly, one of the most actual "continuously-under-development" software OpenSees (2004), which can handle 3D problems for various hysteretic relations, should also be referred herein.

This paper presents a methodology for the non-linear stochastic analysis of three dimensional reinforced-concrete shear wall-frame systems and a developed computer program on the purpose, based on Monte-Carlo simulation technique.

2. Non-linear behavior of elements

During the analysis of the seismic response of R-C elements, the developed program SAR-CWF handles material non-linearity as well as the following items.

- Different yield capacities with respect to positive and negative bending for unsymmetrical cross-sections,
- Effect of axial force on yield capacity of a section (P - δ effect),
- Stiffness and strength degradation during plastic deformations,
- Pinching effect caused by shear forces on moment-curvature relation,
- Finite plastic zone extensions at the end of structural elements.

For the analysis including the below mentioned items, the following essential assumptions are made.

- i. Bernoulli hypothesis is accepted during elastic and plastic deformations.
- ii. Compared to their length, all deformations of elements are small.
- iii. Increments of axial forces and torsional moments depend linearly on the increments of the axial elongation and the angular displacement, respectively.
- iv. Except for shear walls, influence of shear deformations is ignored.
- v. Incremental constitutive moment-curvature relationship with respect to local bending axes of the element is assumed to be decoupled.
- vi. Inertial and linear viscous loading within the element are applied as external statically equivalent nodal loadings.

Hence the behavior of structural elements vary with respect to the internal forces, two different hysteretic models are applied in this study.

2.1 Roufaiel-Meyer hysteretic model for bending

Fig. 1 shows a dimensionless bending moment-curvature relation for structural elements subject to dynamic loading. According to assumption (v), it is obvious that this relation is used independently for all local axes.

In this hysteretic model, the dimensionless bending moment and the corresponding curvature are calculated with the following relation as in Eq. (1).

$$\frac{\partial}{\partial t} m(x, t) = ei\left(\pm\left(\frac{\partial c}{\partial t}\right), m, p\right) \frac{\partial}{\partial t} c(x, t) \tag{1}$$

where

$$m(x, t) = \frac{M(x, t)}{M_y^+(x)} \qquad c(x, t) = \frac{\kappa(x, t)}{\kappa_y^+(x)} \tag{2a}$$

$$ei(x, t) = \frac{EI(x, t)}{EI_{eq}(x)} \qquad EI_{eq}(x) = \frac{M_y^+(x)}{\kappa_y^+(x)} \tag{2b}$$

$M_y^+(x)$ is the yielding moment of a section at positive bending calculated by the effect of static axial force $N^{(s)}$, with zero static bending moment and $\kappa_y^+(x)$ is the corresponding curvature. EI_{eq} can be presented as the equivalent bending stiffness of the concrete section so that $ei(x, t)$ stands for the

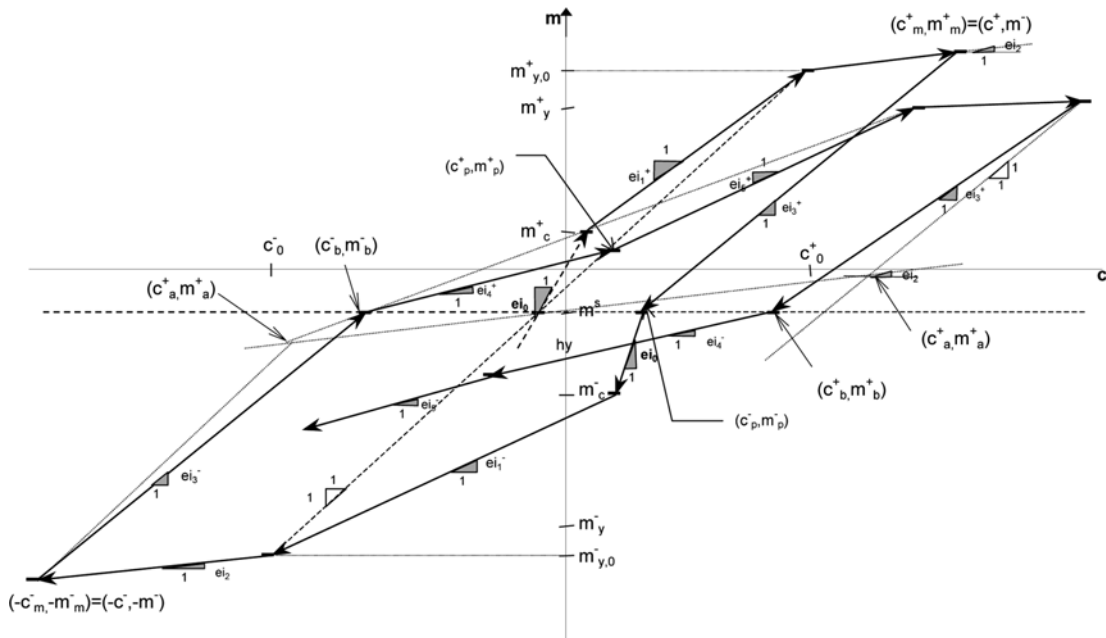


Fig. 1 Roufaiel-Meyer hysteretic model for bending

normalized bending stiffness. The loading and unloading branches on the hysteretic model are controlled by the value of the bending moment $M(x, t)$ and the sign of the corresponding curvature rate

$\frac{\partial}{\partial t} \kappa(x, t)$ where the slopes of those at time t are identified by $\mathbf{p}(x, t)$ parameters. Note that, according

to the model $M_y^+(x)$ and $M_y^-(x)$, $\kappa_y^+(x)$, crack formation moments $M_c^+(x)$ and $M_c^-(x)$, strain hardening value $s(x)$, static bending moment $M^{(s)}(x)$ and the static axial force $N^{(s)}$ are assumed to be known quantities. Control points on the hysteretic model are defined as:

$$m^{(s)}(x) = \frac{M^{(s)}(x)}{M_y^+(x)} \quad (3)$$

$$m_{y,0}^+(x) = 1 - m^{(s)}(x) \quad m_{y,0}^-(x) = \frac{M_y^-(x)}{M_y^+(x)} + m^{(s)}(x) \quad (4)$$

$$m_c^+(x) = \frac{M_c^+(x)}{M_y^+(x)} - m^{(s)}(x) \quad m_c^-(x) = \frac{M_c^-(x)}{M_y^+(x)} + m^{(s)}(x) \quad (5)$$

$$c_0^+ = \begin{cases} 1 - \frac{m^{(s)}}{ei_0} & -M_c^- \leq M^{(s)} \leq M_c^+ \\ \frac{m_{y,0}^+}{(m_{y,0}^+ - m_c^+)} \left[1 - \frac{(m_c^+ + m^{(s)})}{ei_0} \right] & M^{(s)} > M_c^+ \\ m_{y,0}^+ + \frac{m_{y,0}^-}{(m_{y,0}^- - m_c^-)} (m^{(s)} - m_c^-) \left(1 - \frac{1}{ei_0} \right) & M^{(s)} < -M_c^- \end{cases} \quad (6)$$

$$c_0^- = m_{y,0}^+ + m_{y,0}^- - c_0^+ \quad (7)$$

It is assumed that the initial static moment, $M^{(s)}$, is less than the yielding moment of the section. Because of the deformations during the vibration, initial yield capacities $m_{y,0}^+(x)$ and $m_{y,0}^-(x)$ decrease and at a time t , these are described as $m_y^+(x, t)$ and $m_y^-(x, t)$.

The total bending moment $M(x, t) + M^{(s)}(x)$, is defined within six different loading and unloading branches on the model. The dimensionless bending stiffness $ei_0, ei_1^+, ei_1^-, ei_2, ei_3^+, ei_3^-, ei_4^+, ei_4^-, ei_5^+$ and ei_5^- for these branches are:

$$ei_0 = \frac{EI_{uc}}{EI_{eq}} \quad ei_1^+ = \frac{m^+ - m}{c^+ - c} \quad ei_1^- = \frac{m^- - m}{c^- + c} \quad ei_2 = s \quad (8a)$$

$$ei_3^+ = \frac{m_b^+ - m_m^+}{c_b^+ - c_m^+} \quad ei_3^- = \frac{m_b^- - m_m^-}{c_b^- - c_m^-} \quad ei_4^+ = \frac{m_p^+ - m_b^-}{c_p^+ - c_b^-} \quad ei_4^- = \frac{m_p^- - m_b^+}{c_p^- - c_b^+} \quad (8b)$$

$$ei_5^+ = \frac{m^+ - m}{c^+ - c} \quad ei_5^- = \frac{m^- + m}{c^- + c} \quad (8c)$$

where m^+ and m^- are the values of $m(x, t)$ at previous loading or unloading branch and c^+ and c^- are the corresponding curvature ductilities. Therefore, the following relations for positive and negative bending can be written.

$$m^+ = m_y^+ + s \cdot (c^+ - c_0^+) \quad m^- = m_y^- + s \cdot (c^- - c_0^-) \quad (9)$$

The coordinates of pinching points and others can easily be calculated from geometric relations and are given by Roufaiel and Meyer (1987). Therefore, from the hysteretic model, dimensionless bending stiffness $ei(x, t)$ is calculated as:

$$\begin{aligned} ei(x, t) = & ei_0(x, t)[\alpha_0^+(x, t) + \alpha_0^-(x, t)] + ei_1^+(x, t)\alpha_1^+(x, t) + ei_1^-(x, t)\alpha_1^-(x, t) + ei_2(x, t)\alpha_2(x, t) \\ & + ei_3^+(x, t)\alpha_3^+(x, t) + ei_3^-(x, t)\alpha_3^-(x, t) + ei_4^+(x, t)\alpha_4^+(x, t) + ei_4^-(x, t)\alpha_4^-(x, t) \\ & + ei_5^+(x, t)\alpha_5^+(x, t) + ei_5^-(x, t)\alpha_5^-(x, t) \end{aligned} \quad (10)$$

where α_i^\pm are indicator functions having the value of 1 on loading branches or 0 during unloading. The indicator functions are controlled by Heaviside unit-step functions and detailed information can be found in Mørk (1992).

2.2 Strength deterioration

Besides the stiffness degradation caused by dynamic loads, reinforced concrete members also experience strength deterioration. Spalling off concrete cover during a critical level of displacement is one of the measures for the loss of strength (Atalay and Penzien 1975). An approach for the random vibration problem with an empirical characterization of stiffness degradation is also sketched out under an external Gaussian white noise loading by Sobczyk and Trębicki (2000). In this study, a strength deterioration model experimentally developed by Kristensen and Nørgaard (1992) which is based on the former studies of Ma *et al.* (1976), is used. According to the model;

- Strength deterioration starts when the normalized curvatures c^+ or c^- for a section at positive or negative bending exceeds the critical level of spalling curvatures c_s^+ or c_s^- , respectively.
- The value $c_s = \kappa_s / \kappa_y^+ = c_s^+ = c_s^-$ is constant in an element's section.
- Strength deterioration is controlled by utilizing normalized accumulated hysteretic energy $e(x, t)$, from the start time of deterioration until the end of dynamic loading.
- The strength deterioration is considered to be decoupled with respect to the local axes y and z .
- Loss of strength at positive bending leads also a decrease in strength of negative bending which can be defined as isotropic strength deterioration.

The following strength deterioration model $g(e)$, is applied as it is offered with c_s having a mean value of 5 and a coefficient of variation of 10% (Nielsen *et al.* 1989).

$$m_y^+(x, t) = m_{y,0}^+(x) \cdot g[e(x, t)] \quad m_y^-(x, t) = m_{y,0}^-(x) \cdot g[e(x, t)] \quad (11)$$

$$g(e) = \begin{cases} 1 & e \leq e_0 \\ \exp\left(-\frac{e - e_0}{e_1}\right) & e > e_0 \end{cases} \quad (12)$$

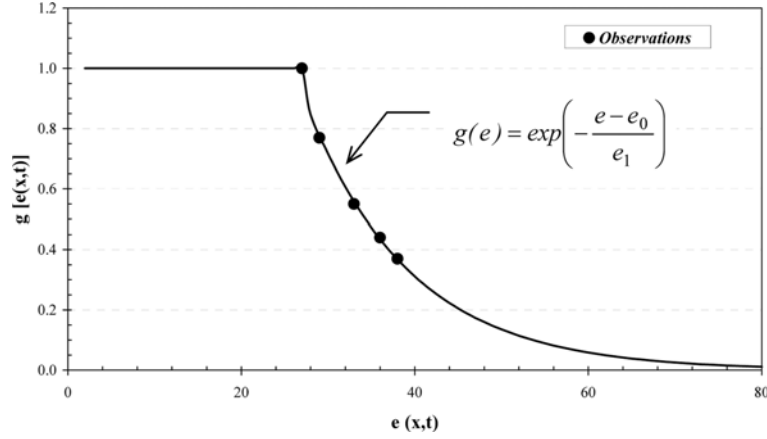


Fig. 2 Strength deterioration - accumulated hysteretic energy relation

The coefficients e_0 and e_1 are the limit value and the decay ratio, respectively in the model. Fig. 2 shows the strength deterioration model with experimentally observed results.

The non-dimensional accumulated hysteretic energy is defined as

$$e(x, t) = \int_{t_0}^t m(x, \tau) dc(x, \tau); \quad t > t_0 \quad (13)$$

where t_0 is the start time of deterioration.

By differentiating Eq. (13), the time varying expression of the accumulated hysteretic energy can be obtained as;

$$\frac{\partial}{\partial t} e(x, t) = m(x, t) \cdot [H(c^+ - c_s) \cdot H(c^+ - c^-) + H(c^- - c_s) \cdot (1 - H(c^+ - c^-))] \frac{\partial}{\partial t} c(x, t) \quad (14)$$

where $H(*)$ is the unit-step function. Since the parameters in the model depend on $\partial c / \partial t$, $m(x, t)$, the current value of $c(x, t)$, the curvature ductilities $c^+(x, t)$ and $c^-(x, t)$ and the non-dimensional accumulated hysteretic energy $e(x, t)$, additional state variables are necessary to be presented as;

$$p^T(x, t) = [c(x, t), c^+(x, t), c^-(x, t), e(x, t)] \quad (15)$$

Using Eq. (9) and Eq. (14) together, the following expression and the initial values can be written.

$$\frac{\partial}{\partial t} \tilde{p} = \begin{bmatrix} 1 \\ H(m - m_y^+ - s(c^+ - c_0^+)) \cdot H\left(\frac{\partial c}{\partial t}\right) \\ -H(-m - m_y^- - s(c^- - c_0^-)) \cdot H\left(-\frac{\partial c}{\partial t}\right) \\ m[H(c^+ - c_s) \cdot H(c^+ - c^-) + H(c^- - c_s)(1 - H(c^+ - c^-))] \end{bmatrix} \frac{\partial c}{\partial t} = f\left(\frac{\partial c}{\partial t}, m, p\right) \quad (16)$$

$$\{p(x, 0)\} = \begin{bmatrix} c(x, 0) \\ c^+(x, 0) \\ c^-(x, 0) \\ e(x, 0) \end{bmatrix} = \begin{bmatrix} c_0(x) \\ c_0^+(x) \\ c_0^-(x) \\ 0 \end{bmatrix} \quad (17)$$

2.3 Origin-Oriented hysteretic model for shear reversals

Incremental shear stiffness properties of reinforced concrete walls are modeled by a tri-linear origin-oriented hysteretic envelope. This model establishes the relation between shear forces and the corresponding shear displacement. In other words, the relation of shear stresses and shear deformations for a wall section is realized.

Fig. 3 shows the origin-oriented hysteretic model used in this study where v_{cr} , v_y and v_u are the cracking, yielding and ultimate shear stresses and γ_{cr} , γ_y and γ_u are the corresponding shear deformations, respectively. Initially, the shear modulus G_0 is assumed to be related with the modulus of elasticity E_c .

G_{cr} is the ratio of shear stress to strain at shear yielding (Hoedajanto 1983). Introducing ν as the Poisson's ratio, ρ is the ratio of transverse reinforcement, n the ratio of elasticity modulus of steel to concrete, A_{sh} as the effective area of wall, h the story height, V shear force of the wall and δ_s as the shear displacement as it is seen in Figs. 4(a) and 4(b), the following equations can be written.

$$G_0 = E_c / [2 \cdot (1 + \nu)] \quad G_{cr} = \rho \cdot n \cdot G_0 \quad (18)$$

$$V = v \cdot A_{sh} \quad \delta_s = \gamma \cdot h \quad v_y = \rho \cdot f_{yk} \quad (19)$$

In the model, the loading branch follows the main skeleton at the beginning. Since the element will behave elastically before cracking, there is no loss in the hysteretic energy. Therefore, the shear

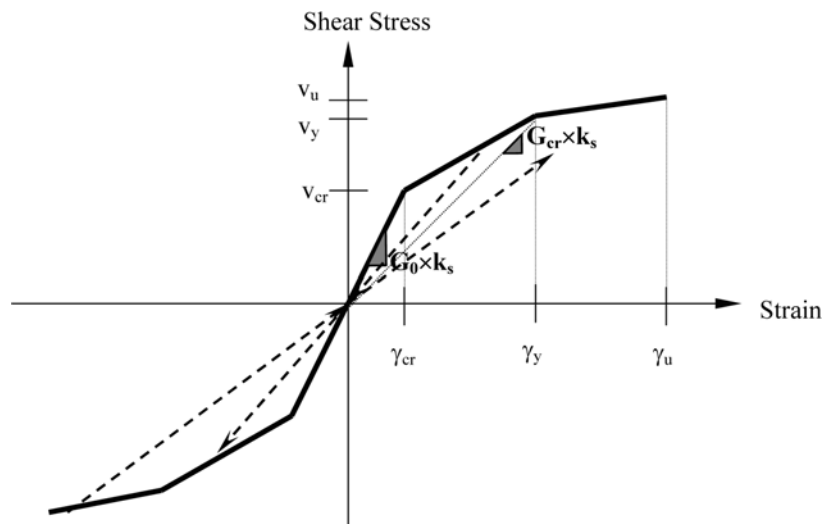


Fig. 3 Origin-Oriented hysteretic model for shear reversals

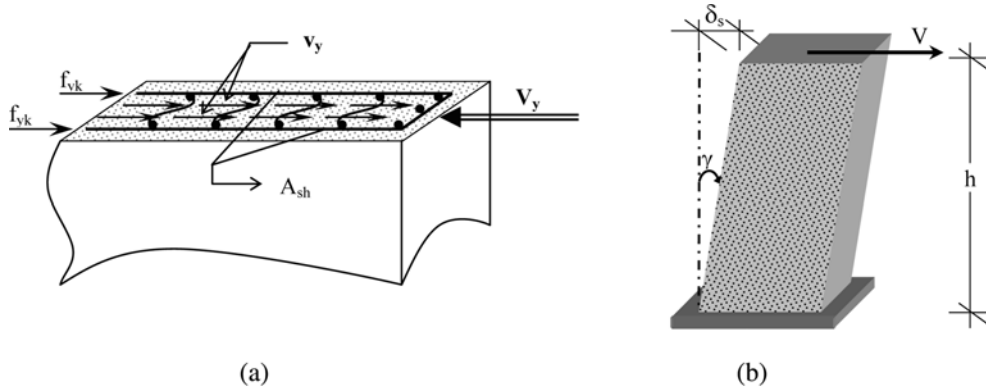


Fig. 4 (a) Shear stresses and reinforcement of a shear wall, (b) Shear deformation versus displacement

stiffness will follow the initial slope during loading and unloading. During the subsequent reloading, the unloading path is followed until the main skeleton is encountered. If unloading occurs before crossing the main curve, the unloading path points toward the origin, if the main skeleton is encountered then the path follows the primary curve. Therefore, the value of shear stiffness, K , varying on loading or unloading branches in the hysteretic model can be calculated depending on the incremental G value as,

$$K = G \cdot \frac{A_{sh}}{h} = G \cdot k_s \quad (20)$$

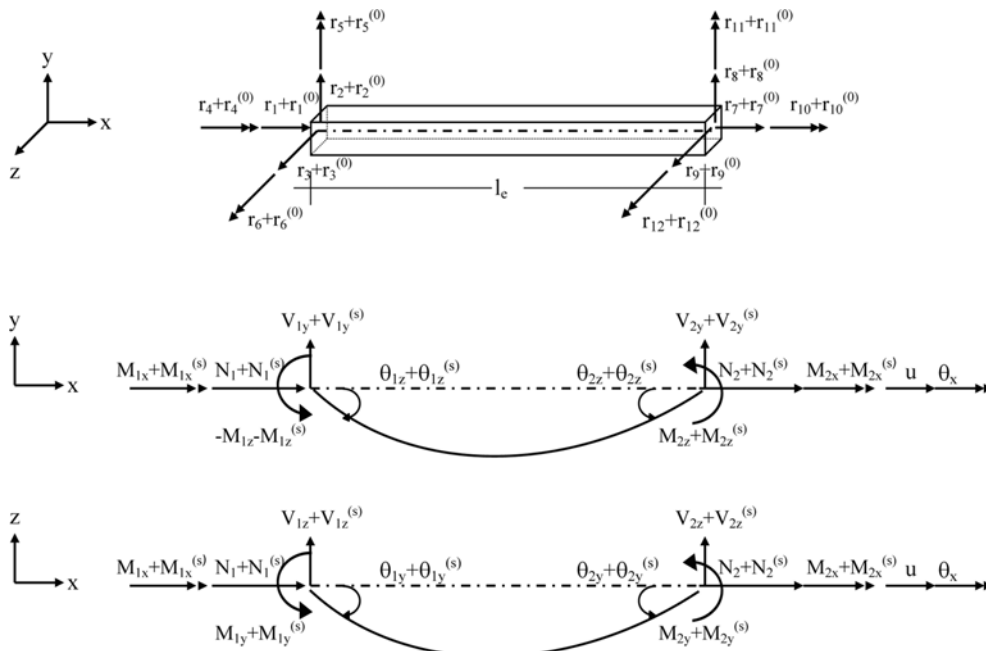


Fig. 5 Nodal displacements and end forces of a beam or a column

3. Analysis of the elements consisting a shear wall-frame system

Considering the differences in compatibility and constitutive relations depending on the characteristic behavioral properties of reinforced concrete members consisting a structural system, beams and columns, tie beams and finally shear walls are handled in three sub-groups.

3.1 Compatibility relations for beams and columns

Fig. 5 shows the displacements and end forces a beam or a column element in the statical equilibrium and the dynamically deformed states where the superscript ^(s) denotes the internal forces before the dynamic loads are applied and ⁽⁰⁾ stands for the stiff-body displaced state.

Therefore, the total nodal displacements, which are referred as external degrees of freedom by Mørk (1992), can be written as

$$\{r_e\}^T = \{r_3 \ r_5 \ r_9 \ r_{11} \ r_2 \ r_6 \ r_8 \ r_{12} \ r_4 \ r_{10} \ r_1 \ r_7\} \quad (21)$$

and the end forces conjugated to $\{r_e\}$ are

$$\{R_e\}^T = \{V_{1z} \ M_{1y} \ V_{2z} \ -M_{2y} \ V_{1y} \ -M_{1z} \ V_{2y} \ M_{2z} \ M_{1x} \ M_{2x} \ N_1 \ N_2\} \quad (22)$$

Because of assumption (iii) in section 2, six of these quantities are sufficient to describe the generalized stresses $\{Q_e\}$.

$$\{Q_e\} = \begin{Bmatrix} \tilde{M}_e^y \\ \tilde{M}_e^z \\ M_e^x \\ N \end{Bmatrix} \quad \text{where} \quad \{M_e^y\} = \begin{Bmatrix} M_{1y} \\ M_{2y} \end{Bmatrix} \quad \{M_e^z\} = \begin{Bmatrix} M_{1z} \\ M_{2z} \end{Bmatrix} \quad M_e^x = M_{1x} = M_{2x} \quad (23)$$

then the nodal displacements will be

$$\{q_e\} = \begin{Bmatrix} \tilde{\theta}_e^y \\ \tilde{\theta}_e^z \\ \theta_e^x \\ u \end{Bmatrix} \quad \text{where} \quad \{\theta_e^y\} = \begin{Bmatrix} \theta_{1y} \\ \theta_{2y} \end{Bmatrix} \quad \{\theta_e^z\} = \begin{Bmatrix} \theta_{1z} \\ \theta_{2z} \end{Bmatrix} \quad (24)$$

Here, u and θ_x signifies the axial elongation and angular displacement, respectively. The generalized nodal displacements $\{q_e\}$ will be referred as internal degrees of freedom. By using the compatibility relation, the rate of $\{r_e\}$ and $\{q_e\}$ are related

$$\{\dot{q}_e\} = [a_e] \cdot \{\dot{r}_e\} \quad (25)$$

where a_e is the compatibility matrix

$$[a_e] = \begin{bmatrix} \tilde{a}_e^y & \tilde{0} & \tilde{0} & \tilde{0} \\ \tilde{0} & \tilde{a}_e^z & \tilde{0} & \tilde{0} \\ \tilde{0} & \tilde{0} & \tilde{a}_e^x & \tilde{0} \\ \tilde{0} & \tilde{0} & \tilde{0} & \tilde{a}_e^x \end{bmatrix} \quad (26)$$

with components

$$a_e^y = \begin{bmatrix} -1/l_e & 1 & 1/l_e & 0 \\ 1/l_e & 0 & -1/l_e & -1 \end{bmatrix} \quad a_e^z = \begin{bmatrix} -1/l_e & -1 & 1/l_e & 0 \\ 1/l_e & 0 & 1/l_e & 1 \end{bmatrix} \quad a_e^x = [-1 \quad 1] \quad (27)$$

3.1.1 Constitutive relations

Incremental constitutive relation of a beam or a column section at a distance of x , can be written due to assumptions (ii) and (iii) as in the following expressions.

$$\frac{\partial N(x, t)}{\partial t} = \frac{AE}{l_e} \frac{\partial u}{\partial t} \quad (28)$$

$$\frac{\partial M_e^x(x, t)}{\partial t} = \frac{GI_x}{l_e} \frac{\partial \theta_x}{\partial t} \quad (29)$$

$$\frac{\partial M_e^{y,z}(x, t)}{\partial t} = EI^{y,z} \left(\pm \left(\frac{\partial \kappa^{y,z}}{\partial t} \right), M^{y,z}, p \right) \frac{\partial \kappa^{y,z}(x, t)}{\partial t} \quad (30)$$

where l_e is the element length, AE is the axial stiffness, GI_x is the torsional stiffness, $EI^{y,z}$ is the bending stiffness with respect to the local axes y and z , $N(x, t)$ is the axial force, $M_e^x(x, t)$ is the torsional moment, $M_e^{y,z}(x, t)$ are the bending moments with respect to local axes y and z , $\kappa^{y,z}(x, t)$ are the corresponding curvatures and $p(x, t)$ is the parameter controlling stiffness and strength deterioration. Fig. 6 shows a beam cross-section with the height h , tensile reinforcement area of A_s and the cover depth of d' for positive bending.

Anyone can write the equilibrium equations for the above section as

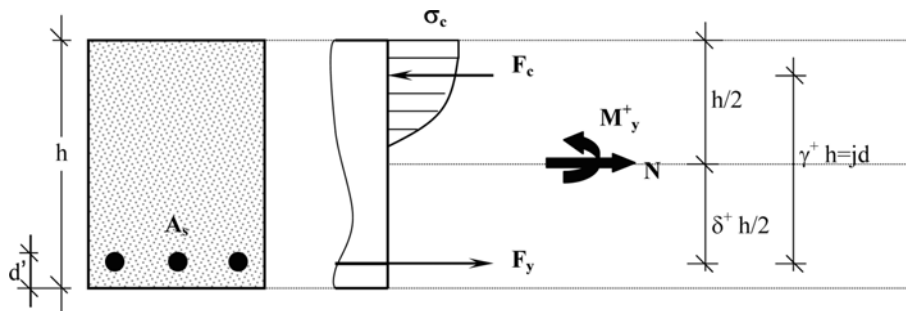


Fig. 6 External forces and internal stresses of a beam element

$$N = F_y - F_c \quad (31a)$$

$$M_y^+ = F_y \cdot (jd) - N \cdot (jd - h/2 + d') \quad (31b)$$

$$= F_y \cdot \gamma^+ h - N \cdot (\gamma^+ - \delta^+/2) \cdot h \quad (31c)$$

$$\gamma^+ = jd/h, \quad \delta^+ = 1 - 2\beta, \quad \beta = d'/h \quad (31d)$$

Since the variation of γ^+ is not significantly sensitive to N , the initial yield moment calculated for zero axial force can be written approximately as,

$$M_{y,0}^+ \cong F_y \gamma^+ h \quad (32)$$

and the contribution of axial force to the yielding at static equilibrium state can be expressed as,

$$M_y^+ = M_{y,0}^+ - N^{(s)} \left(\gamma^+ - \frac{\delta^+}{2} \right) h \quad (33)$$

Same procedure can be applied for negative bending.

$$M_y^- = M_{y,0}^- - N^{(s)} \left(\gamma^- - \frac{\delta^-}{2} \right) h \quad (34)$$

Considering Eq. (23), Eq. (24) and Eq. (25), the relation between the rates $\{\dot{Q}_e(t)\}$ and $\{\dot{q}_e(t)\}$ can be obtained by applying the virtual work principle.

$$\{\dot{Q}_e(t)\} = [k_e(t)] \cdot \{\dot{q}_e(t)\} \quad (35)$$

Here, $\mathbf{k}_e(t)$ is the incremental stiffness matrix of the element with members,

$$[k_e(t)] = \begin{bmatrix} [k_{pl,e}^y] & \tilde{0} & 0 & 0 \\ \tilde{0} & [k_{pl,e}^z] & 0 & 0 \\ \tilde{0} & \tilde{0} & \frac{GI_x}{l_e} & 0 \\ \tilde{0} & \tilde{0} & 0 & \frac{EA}{l_e} \end{bmatrix} \quad (36)$$

Taking $\xi = x/l_e$, the non-linear members of the above matrix can be written as follows.

$$[k_{pl,e}^y] = \frac{EI_{eq}^y}{l_e} \begin{bmatrix} \int_0^1 \frac{(1-\xi)^2}{e^{i^y(\xi,t)}} d\xi & \int_0^1 \frac{(1-\xi)\xi}{e^{i^y(\xi,t)}} d\xi \\ \int_0^1 \frac{(1-\xi)\xi}{e^{i^y(\xi,t)}} d\xi & \int_0^1 \frac{\xi^2}{e^{i^y(\xi,t)}} d\xi \end{bmatrix}^{-1} \quad [k_{pl,e}^z] = \frac{EI_{eq}^z}{l_e} \begin{bmatrix} \int_0^1 \frac{(1-\xi)^2}{e^{i^z(\xi,t)}} d\xi & \int_0^1 \frac{(1-\xi)\xi}{e^{i^z(\xi,t)}} d\xi \\ \int_0^1 \frac{(1-\xi)\xi}{e^{i^z(\xi,t)}} d\xi & \int_0^1 \frac{\xi^2}{e^{i^z(\xi,t)}} d\xi \end{bmatrix}^{-1} \quad (37)$$

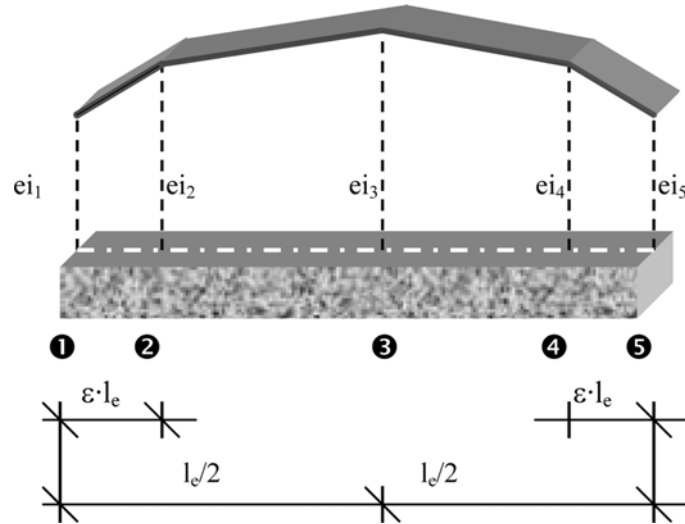


Fig. 7 Variation of non-dimensional bending stiffness

The $ei^v(\xi, t)$ and $ei^z(\xi, t)$, non-dimensional bending stiffnesses are calculated by linear interpolation within five discrete coordinates as seen in Fig. 7.

It should be stated that, ε controls the plastic hinge length.

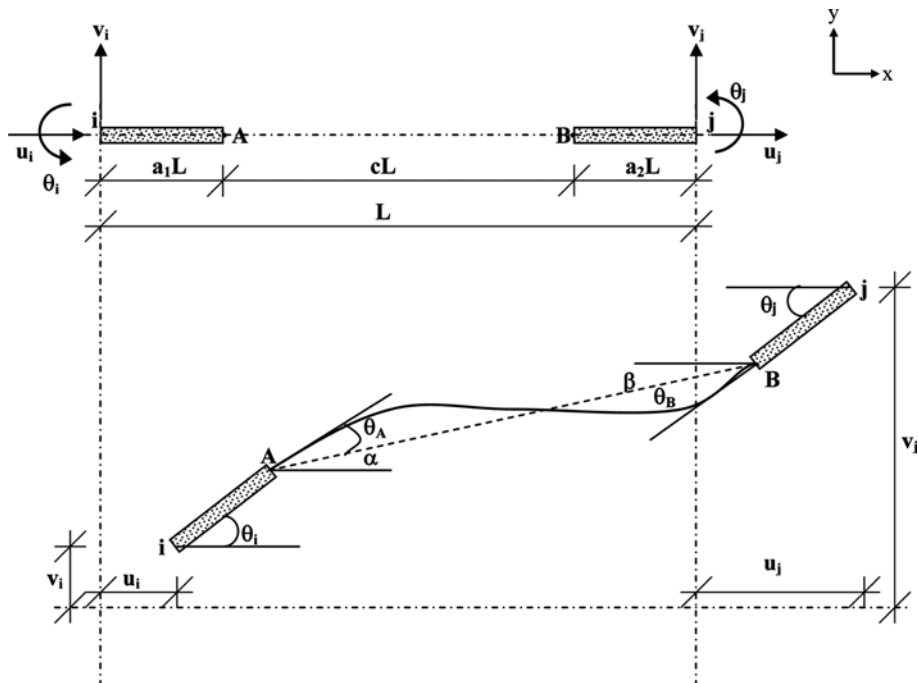


Fig. 8 Nodal displacements of tie beams with rigid supports at both nodes

3.2 Compatibility relations for coupled beams

Although similar nodal displacements and loadings are present in coupled beams, the compatibility relations are different from beams and columns because of the rigid support at one or each end. Fig. 8 illustrates a dynamically deformed tie-beam.

Using the equilibrium equations and assuming $\sin\alpha \approx \alpha$, $\sin\theta_i \approx \theta_i$, $\sin\theta_j \approx \theta_j$ and $\cos\theta_i \approx 1$, the following compatibility matrix B_c , for tie beams can easily be obtained (Taskin 2001).

$$[B_c] = \begin{bmatrix} 1 & 0 & 0 & 0 & 0 & 0 \\ 0 & 1 & a_1L & 0 & 0 & 0 \\ 0 & \frac{1}{cL} & \frac{1-a_2}{c} & 0 & -\frac{1}{cL} & \frac{a_2}{c} \\ 0 & 0 & 0 & 1 & 0 & 0 \\ 0 & 0 & 0 & 0 & 1 & -a_2L \\ 0 & \frac{1}{cL} & \frac{a_1}{c} & 0 & -\frac{1}{cL} & \frac{1-a_1}{c} \end{bmatrix} \quad (38)$$

Therefore, the stiffness matrix $k_{b,e}$ for tie beams is calculated by,

$$[k_{b,e}] = [B_c]^T [k_{el}] \cdot [B_c] \quad (39)$$

3.3 Compatibility relations for shear walls

Wall elements are determined consisting of n number of linear elastic segments having the same length similar in the study of Lopez (1988). Alternatively, all sub-elements have 12 DOF as seen in Fig. 9.

The value of n varies from four for the top stories to 10 for the lower stories. It is assumed that the moment distribution within the story is linear. Since the bending or shear stiffness value may differ for each segment during non-linear effects, the stiffness matrices for each wall segment are to be obtained considering the effect of shear deformations as in Przemieniecki (1968). As given in Fig. 1, modified Roufaiel-Meyer hysteresis model's rules also control the moment-curvature relation of individual segments of wall elements.

Finally, condensed stiffness matrix S_e for the shear wall having 6 DOF at story levels (i) and ($i + 1$) is formed.

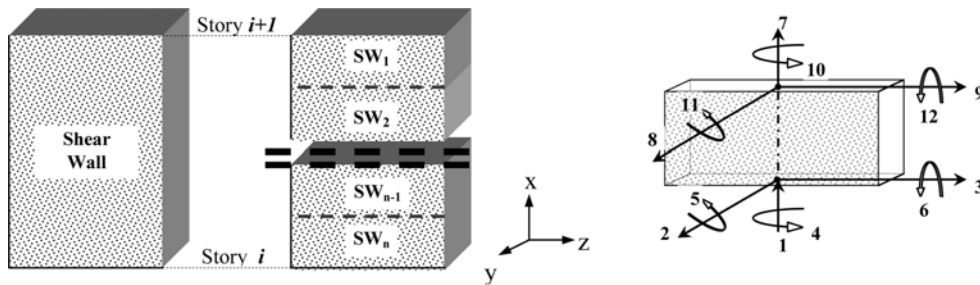


Fig. 9 Division of wall element into segments

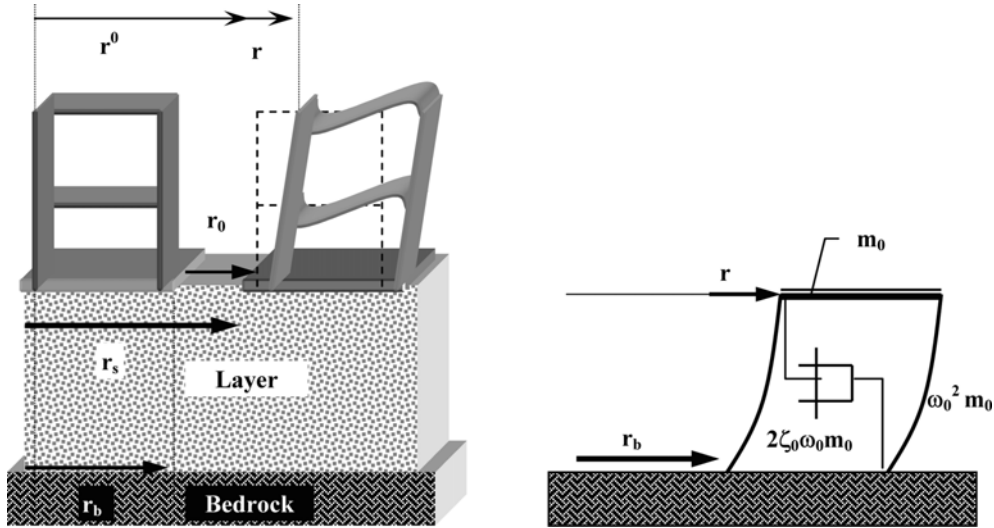


Fig. 10 Modelling of strong motion earthquake

4. Simulation of earthquake motion

The acceleration process at the ground surface is determined as the response process of intensity modulated *Gaussian White Noise*, filtered through a Kanai-Tajimi filter with frequency ω_0 and damping ratio ζ_0 . The displacement of the earth surface r_0 , relative to the bedrock surface is then related to the bedrock acceleration process $\{\ddot{r}_b(t), t \in [0, \infty)\}$ is modeled as in Fig. 10, with the following expression.

$$\ddot{r}_0 + 2\zeta_0\omega_0\dot{r}_0 + \omega_0^2r_0 = -\ddot{r}_b \tag{40}$$

The bedrock acceleration can be obtained from $\ddot{r}_b dt = \beta(t) \cdot dW(t)$ relation, where $W(t)$ is a unit Wiener process (Clough and Penzien 1993). As it was also presented in DiPaola and Muscolino (1990) that, equations of moments of the response statistics for an external Gaussian white noise process were obtained by extending the classical Itô's rule to vectors of random processes and an Itô type differential equation consists of $W(t)$ is called a Wiener vector process. On the other hand, $\beta(t)$ is a deterministic envelope function having the values;

$$\beta(t) = \beta_0 \begin{cases} (t/t_1)^2 & 0 \leq t \leq t_1 \\ 1 & t_1 < t < t_0 + t_1 \\ \exp[-c(t - t_0 - t_1)] & t_0 + t_1 \leq t \end{cases} \tag{41}$$

defined as in Jennings *et al.* (1968).

The acceleration at the ground surface $\ddot{r}_s(t)$ is then be written as,

$$\ddot{r}_s(t) = (\ddot{r}_b + \ddot{r}_0) = (-2\zeta_0\omega_0\dot{r}_0 - \omega_0^2r_0) \tag{42}$$

5. Dynamic analysis of system

The equation of motion in global coordinates is widely known as,

$$[M] \cdot \{\ddot{\mathbf{r}} + \tilde{U}\ddot{\mathbf{r}}_s\} + [C] \cdot \{\dot{\mathbf{r}}\} + [K_{el} + G_* + S] \cdot \{\mathbf{r}\} + [a_{pl}]^T \cdot \{\dot{Q}_{pl}\} = 0 \quad (43)$$

in which \mathbf{r} represents the vector of all translational and rotational DOF, \mathbf{M} mass matrix and \mathbf{C} linear viscous damping matrix determined by Caughey damping model (Caughey and Ma 1982). \mathbf{K} and \mathbf{S} are the stiffness matrices of frame elements and walls, respectively. \mathbf{G}_* stands for geometrical stiffness matrix which is formed if P - δ effect is included. In the expression, the subscripts _(el) and _(pl) define the members in elastic or plastic manner.

Using the compatibility and constitutive relations, the following equations are written,

$$\{\dot{Q}_{el}\} = [k_{el}] \cdot \{\dot{q}_{el}\} \quad \{\dot{Q}_{pl}\} = [k_{pl}(\tilde{Q}_{pl}, \tilde{q}_{pl}, \tilde{p}_{pl})] \cdot \{\dot{q}_{pl}\} \quad (44)$$

where p_{pl} is the additional state variables from plastic elements. Thus, the dynamic equation of motion can be written in the following form considering the acceleration process at the ground surface.

$$\{\dot{q}\}^T \{Q\} = -\{\dot{r}\}^T [M] \{\ddot{\mathbf{r}} + \{U\} \{\ddot{\mathbf{r}}_0 + \ddot{\mathbf{r}}_b\}\} \Rightarrow [M] \{\ddot{\mathbf{r}}\} + [a]^T \{Q\} = [M] \{U\} (2\zeta_0 \omega_0 \dot{r}_0 + \omega_0^2 r_0) \quad (45)$$

5.1 Stochastic equation of motion

The dynamic equation of motion, filter equation and constitutive equations for R-C sections can be combined and written as an equivalent 1st order Stratonovich stochastic differential equation of the following form for further usage: e.g., in the probability distributions to be used in the probabilistic design where lower order moments are required to establish approximate solutions.

$$d\{X(t)\} = \{F\{X\}\}dt + [G(t)] \cdot d\{W(t)\} \quad (46)$$

$$\{X\}^T = \{\{r\} \ \{\dot{r}\} \ r_0 \ \dot{r}_0 \ \{Q_{pl}\} \ \{pl_p\}\}^T \quad (47)$$

$$\{F\{X\}\} = [A\{X\}] \cdot \{X\} + [K(\{Q_{pl}\}, [a_{pl}] \cdot \{\dot{r}\}, \{p_{pl}\})] \cdot [a_{pl}] \cdot \{\dot{r}\} \quad (48)$$

$$[G(t)] = [\tilde{0} \ \tilde{0} \ 0 \ -\beta(t) \ \tilde{0} \ \tilde{0}]^T \quad (49)$$

Above \mathbf{X} is the state vector, $\mathbf{F}(\mathbf{X})$ is the drift vector, and $\mathbf{G}(t)$ is the diffusion matrix. The drift vector $\mathbf{F}(\mathbf{X}, t)$ does only depend on explicitly on time if the filter coefficients are time-dependent. The diffusion vector $\mathbf{G}(t)$ is independent of the state vector $\mathbf{X}(t)$. Finally, first order Stratonovich differential equation is solved by a 4th order Runge-Kutta scheme for the response statistics of the system. Although Ito's and Stratonovich's integral interpretations of stochastic integrals coincide theoretically and even if dynamic system is in the case of excitations only, solutions may be differed according to numerical integration procedures (Kloeden and Platen 1992).

5.2 System reduction

Since the time needed for calculations with the developed software depends on the dimension of the state vector $\mathbf{X}(t)$ which is dependent of the dimension N of the global displacement vector \mathbf{r} and the plastic degree-of-freedom \mathbf{q}_{pl} , a system reduction scheme based on the truncated expansion of the eigenmodes of the undamaged structure is implemented as Mørk and Nielsen (1991).

$$\{r(t)\} \cong \{\Phi\}^1 \cdot y_1(t) + \{\Phi\}^2 \cdot y_2(t) + \dots + \{\Phi\}^n \cdot y_n(t) = [\Phi] \cdot \{y(t)\} \quad n \leq N \quad (50)$$

where

$$[\Phi] = [\{\Phi\}^1 \ \{\Phi\}^2 \ \dots \ \{\Phi\}^n] \quad [y]^T = [y_1(t) \ y_2(t) \ \dots \ y_n(t)] \quad (51)$$

It should be noticed that, by applying $n \leq N$ to global displacement vector, elastic degrees of freedom are eliminated and the plastic degrees of freedom are maintained. Eigenmodes and the corresponding eigenfrequencies are obtained from the eigenvalue problem with Jacobi iteration.

$$[K_{el} + G_* + S] \cdot \{\Phi\}^i = \omega_i^2 \cdot [M] \cdot \{\Phi\}^i \quad i = 1, 2, \dots, n \quad (52)$$

Therefore, the modal coordinates for the first n modes containing the non-linear behavior and for the rest with elastic behavior can be written as,

$$\{y_I\}^T = [y_1 \ \dots \ y_n] \quad \{y_{II}\}^T = [y_{n+1} \ \dots \ y_N] \quad \{y\} = \begin{bmatrix} \{y_I\} \\ \{y_{II}\} \end{bmatrix} \quad (53)$$

and the corresponding orthonormalized modes will be,

$$\{\bar{\Phi}\} = \{\{\bar{\Phi}_I\} \ \{\bar{\Phi}_{II}\}\} \quad (54)$$

When the same procedure is applied to the corresponding constitutive relations, the dynamic system equation turns out to be

$$\{\ddot{y}_I\} + [c_I] \cdot \{\dot{y}_I\} + \{\bar{\Phi}_I\}^T [a_I]^T [K_I] \cdot [a_I] \cdot \{\bar{\Phi}_I y_I + \bar{\Phi}_{II} y_{II}\} + \{\bar{\Phi}_I\}^T [a_I]^T \{Q_I\} = \{\bar{\Phi}_I\}^T \{f(t)\} \quad (55)$$

$$\{\bar{\Phi}_{II}\}^T [a_{II}]^T [K_{II}] \cdot [a_{II}] \cdot \{\bar{\Phi}_I y_I + \bar{\Phi}_{II} y_{II}\} + \{\bar{\Phi}_{II}\}^T [a_{II}]^T \{Q_{II}\} = \{\bar{\Phi}_{II}\}^T \{f(t)\} \quad (56)$$

If the quasi-static modal coordinates in above are ignored, then the equation of motion can be written as;

$$\{\ddot{y}_I\} + [c_I] \cdot \{\dot{y}_I\} + [k_I] \cdot \{y_I\} + \{\bar{\Phi}_I\}^T [a_I]^T \{Q_I - Q_{I,el}\} = \{\bar{\Phi}_I\}^T \{f(t)\} \quad (57)$$

6. Numerical examples

Although the nonstationary response of large linear FE-models under stochastic loading is presented by Schuëller *et al.* (2003), the examples for frame-walled structures, representing

nonlinear stochastic behavior is relatively very rare. For demonstrating the capabilities of the developed software, SAR-CWF, to predict the actual seismic response of RC structures, computations are carried out for two different model-building structures. In 1982, within the framework of a joint U.S-Japan research project, test series for 7-story RC frame-wall buildings were carried out (including pseudo dynamic tests) in Tsukuba, at Building Research Institute (Kabeyasawa *et al.* 1983). The results of these experiments represent very important material for checking the suitability of different mathematical models for the analysis and design of buildings in seismic regions (Fajfar and Fischinger 1987). The second structure is considered for Monte-Carlo simulation model as a five-story RC Frame-wall model structure subjected to a number of 100 simulated strong ground motions.

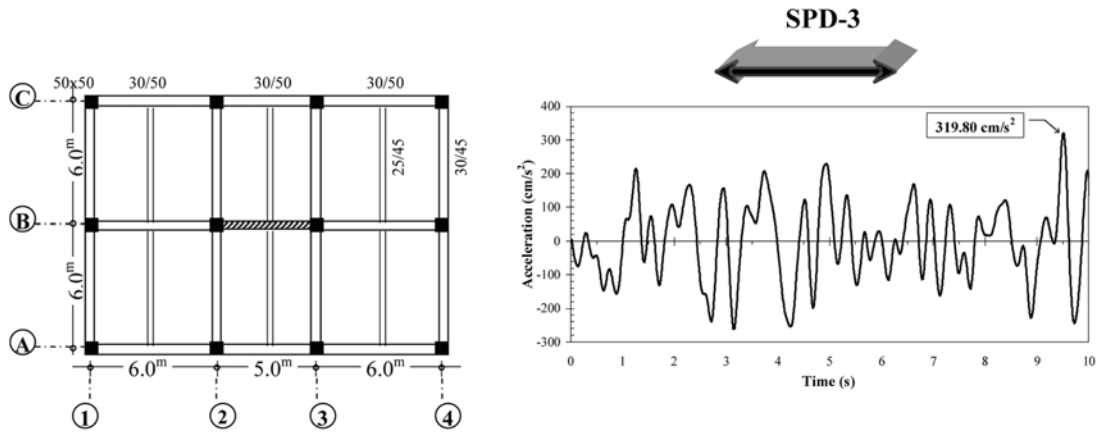


Fig. 11 Floor plan and strong motion history of the BRI building

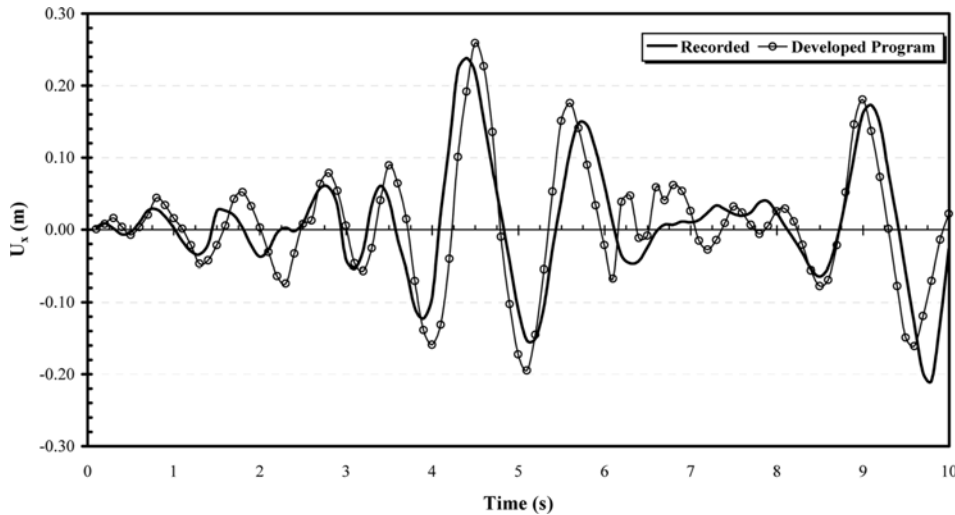


Fig. 12 Top story displacement-time history comparison of the 7 story BRI full-scale test structure

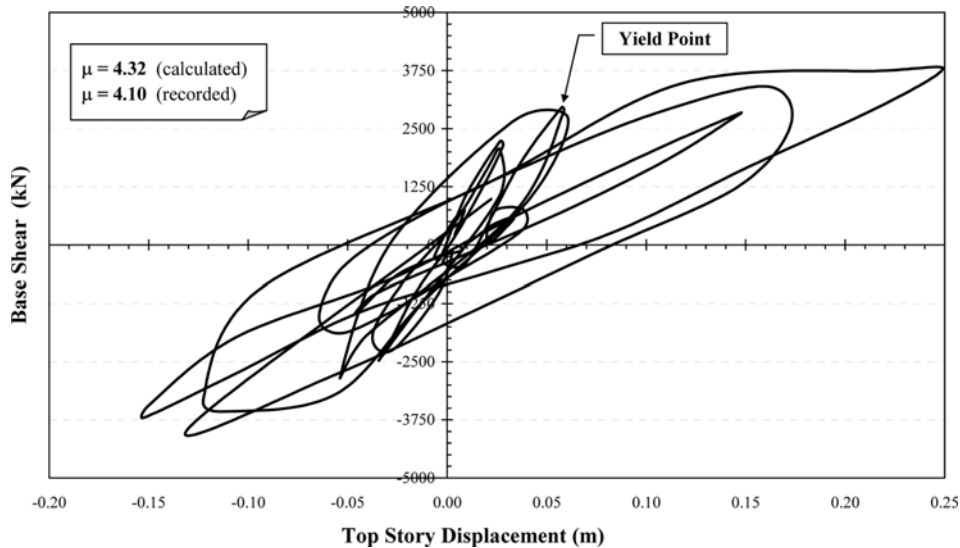


Fig. 13 Determination of the displacement ductility for the BRI test-structure

6.1 Experimentally investigated building example

The above-mentioned BRI full-scale test-structure was investigated as a numerical test and control input structure with its original loading history data obtained by the removal of high frequency components of Taft 1952 EW record (SPD-3) by the developed computer program SAR-CWF. Fig. 11 shows the floor plan, acceleration-time history of the modified strong group motion and loading direction of the related building.

Reinforcement detailing, cross-sectional dimensions, elevation details and other section characteristics such as moment of inertia, yielding moments and corresponding curvatures, etc. of this full-scale building can be found in Midorikawa and Kitagawa (1984). Although single record is applied to this building, it is aimed to illustrate the capabilities of the developed computer program to obtain resembling results, such as response histories for story displacements as given in Fig. 12.

Although the complete dynamic output is not presented herewith, it is also exhibited that the developed computer program is successful at estimating the time and magnitude of peak response values, base shear, overturning moment as well as the displacement ductility, locations and formation of plastic hinges, which have been presented in Taskin and Hasgür (2003). As an example herein, roof displacement versus base-shear variation is plotted in Fig. 13 to obtain the displacement ductility, which is calculated as 4.32 by the use of SAR-CWF and reported as 4.10 after the experiments. Furthermore, the calculated elastic periods $T_{0,1} = 0.46$ s and $T_{0,2} = 0.12$ and the corresponding average test values, $T_{0,1-av} = 0.44$ s and $T_{0,2-av} = 0.12$ s for the first two modes are observed to extend as expected, to $T_1 = 0.87$ s and $T_2 = 0.18$ s according to the calculations and $T_{1-av} = 0.85$ s and $T_{2-av} = 0.18$ s according to the measurements (Kabeyasava *et al.* 1983).

6.2 Model building

Even though it might be possible to generate larger sample sizes depending on the developments

in computing technology, the second numerical example presented herein is a stochastic implication of a generic five-story, shear wall-frame model structure, employing parallel processing based on MC simulation as in Spencer and Bergman (1993) or Johnson *et al.* (1995). The structure is subjected to 100 independent realizations of strong ground motions, with an intensity modulated Gaussian white noise process filtered through a Kanai-Tajimi filter.

6.2.1 Structural properties

Depending on dramatic time increment of computational demands, the idealized model structure is selected relatively simple, having two bays, therefore relatively less joints in both directions with a shear-wall at the middle in x - x direction as seen in Fig. 14. In this 5-story frame-wall structure, the height of the ground story is 4.0 m and the rest are 3.0 m making a total height of 16.0 m. Dimensions of the beam sections are 0.25 m by 0.50 m and the wall sections are 0.25 m by 2.50 m for all stories.

Considering the unit weight of reinforced concrete as $\gamma_c = 25 \text{ kN/m}^3$, modulus of elasticity for concrete as $E_c = 2.85 \times 10^7 \text{ kN/m}^2$, Poisson's ratio of $\nu = 0.20$ and the structural damping ratio

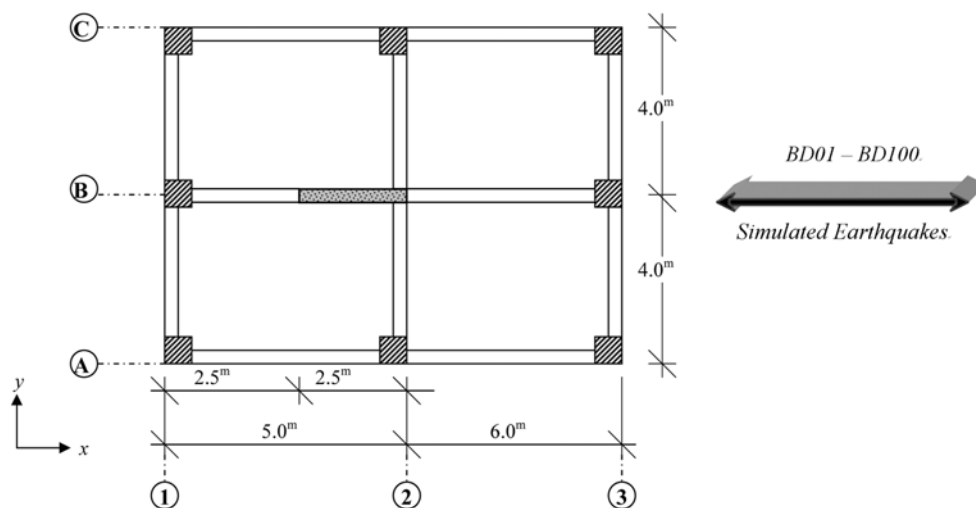


Fig. 14 Floor plan of the example model building

Table 1 Sectional characteristics for local y - y axis

Sec	I^x ($\times 10^{-3} \text{ m}^4$)	I_{eq}^y ($\times 10^{-3} \text{ m}^4$)	A ($\times 10^{-1} \text{ m}^2$)	δ^+	δ^-	γ^+	γ^-	M_u^+ (kNm)	M_u^- (kNm)
1	8.33	5.83	2.68	0.93	0.93	0.78	0.78	314	314
2	3.41	2.40	1.72	0.92	0.92	0.79	0.79	172	172
3	1.08	0.76	0.96	0.89	0.89	0.80	0.80	134	134
4	9.64	3.51	6.53	0.83	0.83	0.76	0.76	583	583
5	9.64	3.47	6.49	0.82	0.82	0.77	0.77	500	500
6	9.64	3.47	6.49	0.82	0.82	0.77	0.77	424	424
7	1.82	0.34	1.29	0.86	0.86	0.79	0.79	23	23
8	1.82	0.34	1.29	0.86	0.86	0.79	0.79	23	23

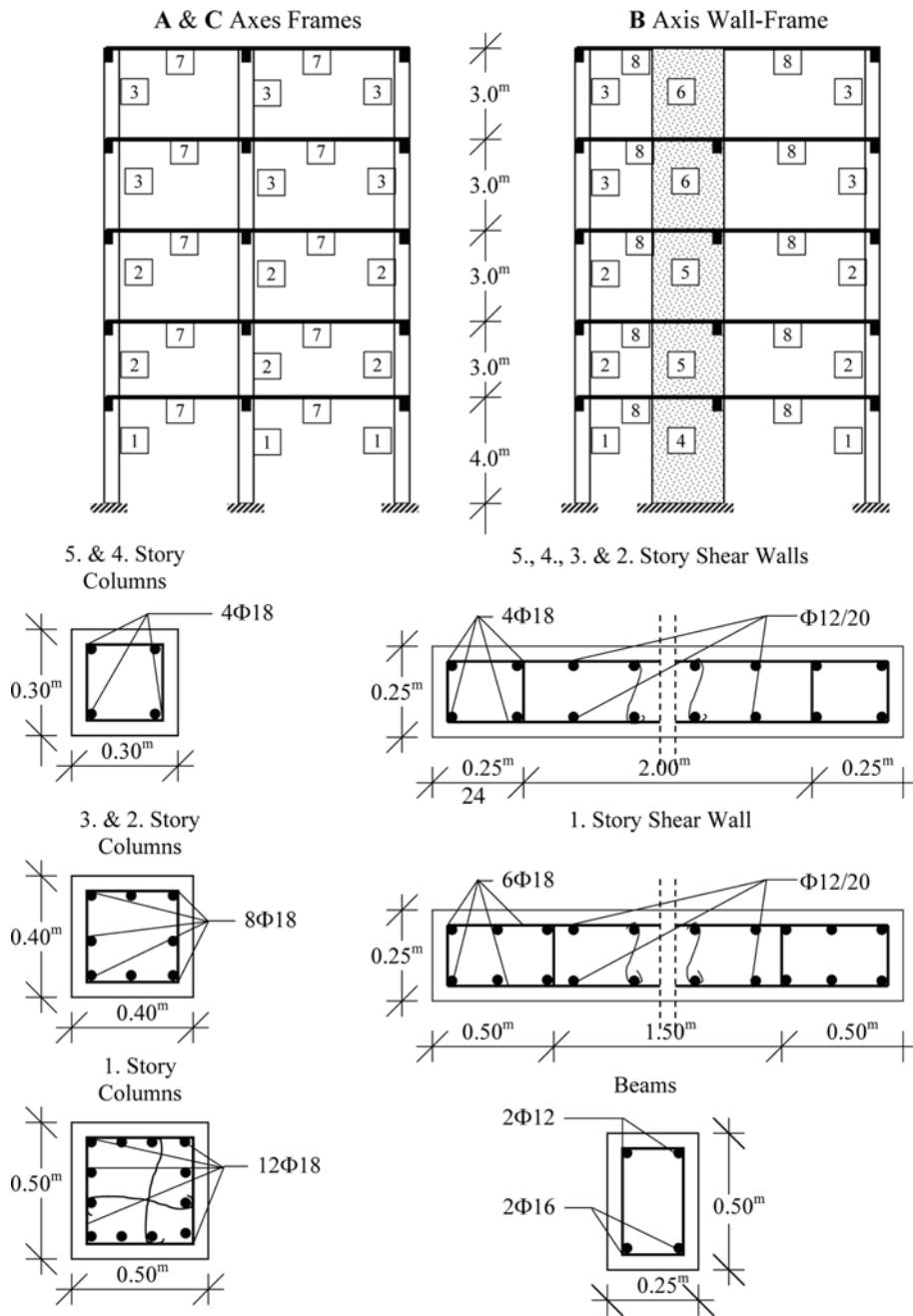


Fig. 15 Elevation, cross-sectional properties and reinforcement details of the structure

$\xi = 0.05$, following characteristic properties for the sections numbered as in the elevation in Fig. 15 are calculated and listed in Tables 1, 2 and 3 for local y - y , z - z directions and for shear walls, respectively. Nevertheless, the reinforcement within the walls is differing depending on the requirement of the Turkish Earthquake Resistant Design Code (1997). Cross-sectional dimensions of

Table 2 Sectional characteristics for local z-z axis

Sec	I^x ($\times 10^{-3} \text{ m}^4$)	$I^{z_{eq}}$ ($\times 10^{-3} \text{ m}^4$)	A ($\times 10^{-1} \text{ m}^2$)	δ^+	δ^-	γ^+	γ^-	M_u^+ (kNm)	M_u^- (kNm)
1	8.33	5.83	2.68	0.93	0.93	0.78	0.78	314	314
2	3.41	2.40	1.72	0.92	0.92	0.79	0.79	172	172
3	1.08	0.76	0.96	0.89	0.89	0.80	0.80	134	134
4	9.64	345.70	6.53	0.83	0.83	0.70	0.70	2966	2966
5	9.64	343.90	6.49	0.82	0.82	0.69	0.69	2587	2587
6	9.64	343.90	6.49	0.82	0.82	0.69	0.69	1998	1998
7	1.82	1.39	1.29	0.93	0.95	0.78	0.79	62	35
8	1.82	1.39	1.29	0.93	0.95	0.78	0.79	62	35

Table 3 Sectional characteristics of RC walls

V_c (kN)	V_y (kN)	V_u (kN)	δ_y ($\times 10^{-2} \text{ m}$)	δ_u ($\times 10^{-2} \text{ m}$)
490	1240	1585	1.51	1.57

the columns are varying from 0.30 m by 0.30 m to 0.50 m by 0.50 m.

It should be emphasized that the sectional characteristics are calculated prior to cracking and considering the contributions of rebar amounts within each element, having an ultimate strain level of $\epsilon_{cu} = 0.004$ for concrete. Moreover, parabolic stress distribution is assumed for a strain level of $\epsilon_c = 0.002$ followed by constant stresses until the ultimate strain level of concrete is applied while linear elastic strain-stress relation is considered for reinforcing steel.

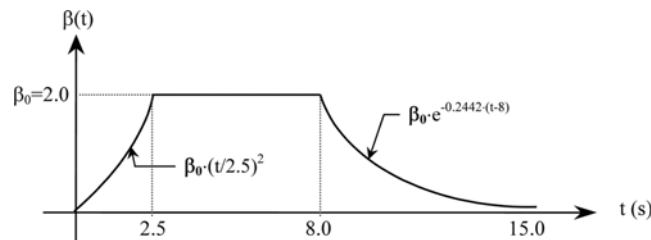


Fig. 16 Deterministic envelope function used for obtaining simulated strong motions

Table 4 Mean value, standard deviation and coefficient of variation of peak ground accelerations

	Simulated accelerations (BD-01~BD-100)
$\mu (a_{max}) \text{ cm/s}^2$	524.6
$\sigma (a_{max}) \text{ cm/s}^2$	11.8
$\sigma/\mu (a_{max})$	0.023

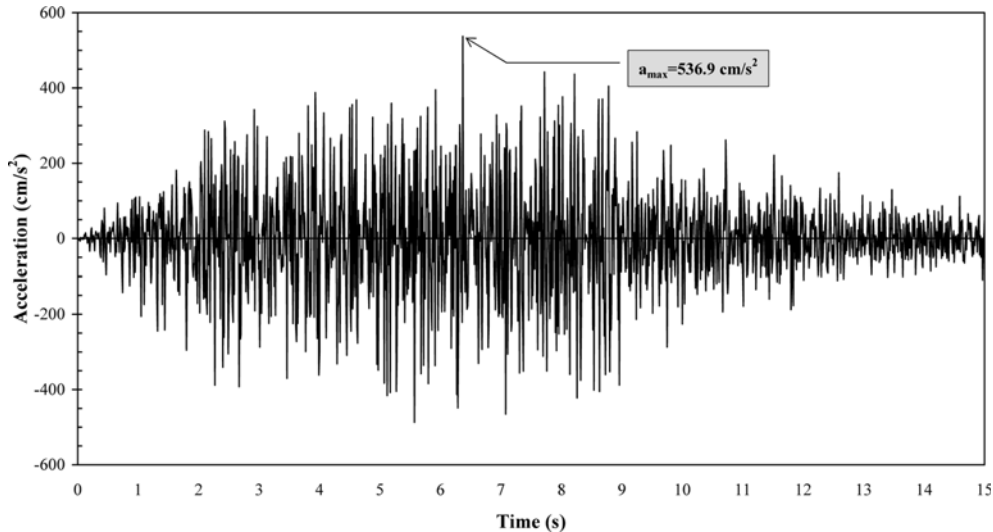


Fig. 17 BD-01 simulated strong motion accelerogram of the ensemble

6.2.2 Simulation of the strong ground motions and the nonlinear dynamic analyses

Kanai-Tajimi filtered white-noise having a power spectral density function intensity of $S_0 = 83.3 \text{ cm}^2/\text{s}^3$ is used for obtaining the stochastic strong motion histories. Considering the parameters for the filter $\zeta_0 = 0.60$ as the damping ratio and an angular frequency of $\omega_0 = 31.2$, simulated earthquake motions with duration of 15 seconds are obtained by multiplying the filtered data with properly modified envelope function given in Fig. 16 (Clough and Penzien 1993).

As a sample from the simulated strong ground motions, for which Table 4 shows the (μ) -mean, (σ) -standard deviation and (σ/μ) -coefficient of variation of the peak ground accelerations of the ensemble, BD-01 motion, having a peak acceleration of 536.9 cm/s^2 and a Housner Intensity of $SI_{0.20} = 164.2 \text{ cm}$, is plotted in Fig. 17.

Since it is aimed to obtain non-linear behavior of the structure, the generation of simulated strong ground motions is forced to represent the strength of destructiveness. To illustrate the severity of these strong motions, it should be emphasized that the $SI_{0.2}$ of given BD-01 accelerogram is 1.77 times stronger than that of El Centro 1940 NS record and is 0.83 times weaker than that of Erzincan-NS 1992 record (Hasgür 1997).

During the dynamic analysis of the example structure, a time step of 0.005 sec is considered. Furthermore, the control parameter for the location of plastic hinges, ε , is taken as 0.10, a strain hardening value of $s(x) = 0.10$ and strength deterioration parameters $e_0 = 26$ and $e_1 = 12$ are used during the computations. Expected value and standard deviation variations are obtained for the top three stories and plotted in Fig. 18 and Fig. 19, respectively, after a total run for 100 realizations of simulated earthquake ground motions.

Figs. 18 and 19 illustrate the expected value of the maximum top story displacement as 0.166 m with a standard deviation of 0.0702 m at time $t = 5.92 \text{ sec}$ after 100 realizations of strong motions. As expected, there is a decrement in these values for the lower stories like 0.146 m and 0.111 m as the story displacements, 0.0621 and 0.0468 for their standard deviations for the fourth and the third stories, respectively. Evaluation of Fig. 19 illustrates that the mean value of $\sigma(U_x)$ for the top story is increasing for the strong motion part, $2.5 \text{ s} \leq t \leq 8.0 \text{ s}$ which has been calculated as 63 mm while

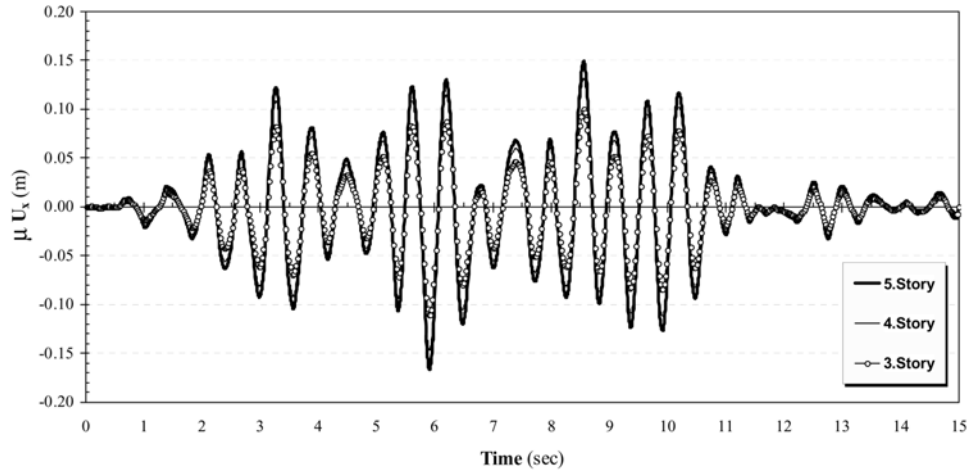


Fig. 18 Time variations of ensemble averages for the displacements of top three stories after 100 simulations, $\mu(U_x)$

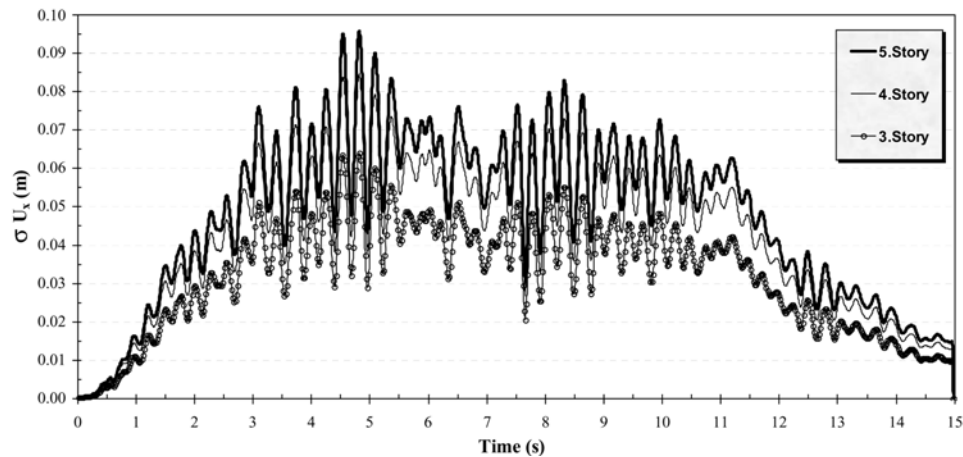


Fig. 19 Time variations of ensemble standard deviations for the displacements of top three stories, $\sigma(U_x)$

it turns out to be 47 mm regarding to the total duration of motion. Following Fig. 20 shows a comparison made to illustrate the variation of the mean top-story displacement history, considering a number of sampling of 2, 40 and 100, respectively.

It is clearly shown that, the mean and the standard deviation variations of the response of the structure decrease for the increasing number of simulations. Abrupt changes are observed for the time variations of the mean values of the top story displacement for smaller sampling sizes while smoother mean displacements are obtained for greater sampling sizes as for $n_{sim} = 100$. Other than the story displacements, the expected value and standard deviation variations of element internal forces are of interest. The following Figs. 21 and 22 show the expected value histories of the bending moment for the bottom A-1 axes column and shear force in the bottom story RC wall, respectively.

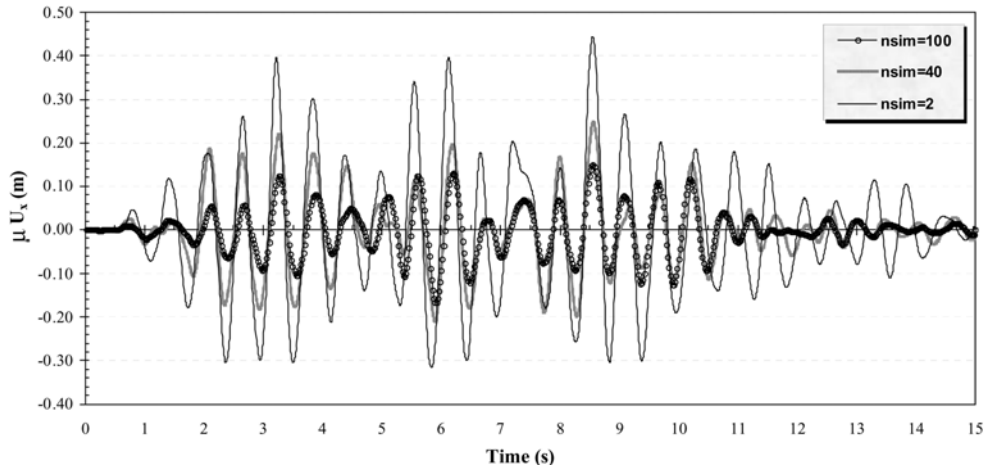


Fig. 20 Time variations of top-story displacements for nsim = 2, 40 and 100, respectively

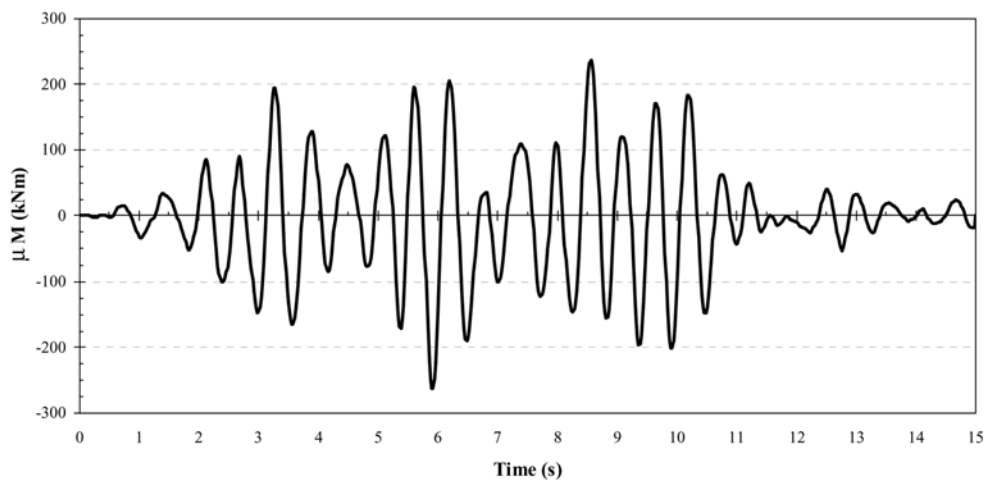


Fig. 21 Time variations of ensemble averages for the bending moment in the bottom A-1 column, $\mu(M_{c-x})$

The results might be compared with the seismic code requirements in the probabilistic sense. For instance, as a result, it is clearly seen that the expected total displacement of the top story is not exceeded extremely according to the Turkish earthquake design code (1997) requirement. Nevertheless, the probability of the nonlinear roof displacement being exceeded under these severe earthquake conditions according to same seismic design code requirement seems to be low. Assuming normal distribution for story displacements with an allowable nonlinear roof displacement value of $0.02 \cdot h_{tot}$, where h_{tot} is the total height of the building, above mentioned probability might be calculated as 1.4% based on the ensemble statistical quantities at $t = 5.92$ s of the excitation. In this case, the basic design criteria met with an acceptable confidence level for the application of the ensemble of such strong ground motions.

For the bottom A-1 column, the expected value of the maximum bending moment is found out to be 263.0 kNm with a standard deviation of 0.264 kNm. This value is found out to be slightly greater than the yield moment of the column which is $M_y = 256.1$ kNm. The maximum values for

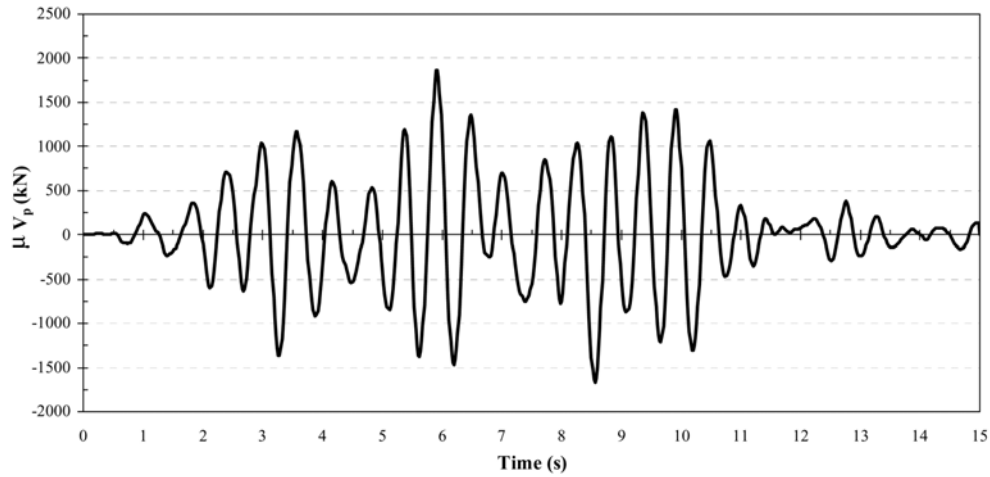


Fig. 22 Time variations of ensemble averages for the shear force in the bottom RC wall, $\mu(V_{sw})$

the bending moment and shear force are expected to be 2672.3 kNm, being slightly less than the yielding value of 2712 kNm and $V_{\max} = 1866.6$ kN, almost 50% more than the $V_y = 1240$ kN for the RC wall in the bottom story.

It is observed for the entire structure that under the effect of such earthquakes, all of the members crack within the first 0.1 seconds and most of them experience yielding after 1.5 seconds. Depending on the results of the calculations, plastic hinge formations in the beams first start at their connections with the shear walls and later proceed in the other node. Plastic hinge formations are also expected for the first story columns and the shear wall, which might lead to collapse due to story failure of the mechanism.

7. Conclusions

A computer program, for which the capabilities have been proven in Taskin and Hasgür (2003), by comparing the calculations and the experimental records of a well-known full-scale structure tested during the US-Japan Co-Operative Research Program in Tsukuba - BRI in 1982 is developed for the non-linear stochastic analysis of 3D RC shear wall-frame structures. In the program, the properties of unsymmetrical cross-sections with different yield capacities, interaction of bending moments and axial forces, stiffness and strength degradation due to plastic deformations, pinching effect of moment-curvature relation and finite extensions of plastic hinges are taken into consideration. Applications of an extended version of Roufaiel-Meyer hysteretic model for bending and Origin-Oriented hysteretic model for shear reversals are performed by carrying out the constitutive relations for different types of structural members. A system reduction scheme based on a truncated expansion of the eigenmodes of the undamaged structure has been realized. Finally, by gathering the dynamic equation of motion, filter equation and constitutive relations, first order Stratonovich stochastic differential equation for the system is obtained as an application of the structural dynamics theory in the means of a statistical approach for performing a probabilistic design procedure.

A comparison of Bolu NS record of Düzce (Turkey) November 12, 1999 earthquake with its $SI_{0.2} = 153$ cm for the cut-off amplitude 529 cm/s^2 instead of the original peak of 807 cm/s^2 , exhibits almost equal strength characteristics to the sample simulated earthquake acceleration of BD-01. The values for the story displacements and their standard deviations are obtained as time histories as illustrated in Figs. 17 and 18 and comparisons for different number of simulations are realized as well. The ensemble averages of the internal force variations for some of the critical structural elements are also investigated. Depending on the expected values of story displacements, yielding of many elements and internal forces exceeding the ultimate capacity of some members, the structure is found to experience moderate to severe damage under the effect of the selected type of earthquake loads. It should be accentuated that the strong motion characteristics are of great importance in the level of the performance of any structure as well as the system ductility and structural load carrying capacity. This study should also be considered as a basis for more enhanced nonlinear demand of such ground motion earthquakes generated at the near fault even for wall-framed structures in probabilistic sense.

On the other hand, various procedures to extent the applicability and to increase the efficiency of Monte Carlo simulation for the analysis of complex dynamical systems, to utilize 'distance controlled' MCS procedure seems to be as a most promising work to increase efficiency of MC simulation for future development of this study.

Acknowledgements

Authors would like to thank Prof. Dr. Søren R.K. Nielsen and Dr. Kim J. Mørk for their valuable interests and fruitful communications, which are the inspiration and the start point of this study. The financial support provided by Aalborg University during the visit of the first author is also appreciated.

References

- Atalay, M.B. and Penzien, J. (1975), "The seismic behavior of critical regions of reinforced concrete components as influenced by moment, shear and axial forces", Report of EERC, EERC-75-19, University of California, Berkeley, California.
- Aydan, Ö., Ulusay, R., Hasgür Z. and Hamada, M. (1999), "The behaviour of structures built on active fault zones in view of actual examples from the 1999 Kocaeli and Chi-Chi earthquakes", *Proc. of the ITU-IAHS Int. Conf. on the Kocaeli Earthquake* 17 August 1999, Istanbul, November, 131-142.
- Baber, T.T. and Wen, Y.K. (1979), "Random vibration of hysteretic degrading structures", *Engineering Mechanics, Proc. 3rd Engrg Mechanics Division Specialty Conf.*, ASCE, NY, 51-54.
- Bouc, R. (1971), "Model mathématique d'hysteresis" *Acustica*, **24**, 16-25.
- Casciati, F. and Faravelli, L. (1989), "Biaxial damage assessment", *Proc. of the Structures Congress '89: Seismic Engineering: Research and Practice*, ASCE, San Francisco, 497-506.
- Casciati, F. and Faravelli, L. (1989), "Stochastic equivalent linearization for 3-D frames", *J. Eng. Mech.*, ASCE, **114**(10), 1760-1771.
- Caughy, T.K. and Ma, F. (1982), "The steady-state response of a class of dynamical systems to stochastic excitations", *J. Appl. Dyn.*, **49**, 629-633.
- Clough, R.W. and Johnston, S.B. (1966), "Effect of stiffness degradation on earthquake ductility requirements", *Proc. of Japan Earthquake Engineering Symposium*, Tokyo.

- Clough, R.W. and Penzien, J. (1993), *Dynamics of Structures*, McGraw-Hill Book Company, NY.
- D'Ambrisi, A. and Filippou, F.C. (1999), "Modeling of cyclic shear behavior in RC members", *J. Struct. Eng.*, ASCE, **125**(10), 1143-1150.
- DiPaola, M. and Muscolino, G. (1990), "Differential moment equations of FE modeled structures with geometrical non-linearities", *Int. J. of Non-Linear Mechanics*, **25**(4), 363-373.
- ElMandooh Galal, K. and Ghobarah, A. (2003), "Flexural and shear hysteretic behaviour of reinforced concrete columns with variable axial load", *Eng. Struct.*, **25**(11), 1353-1454.
- Emam, H.H., Pradlwarter, H.J. and Schuëller, G.I. (2000), "A computational procedure for the implementation of equivalent linearization in finite element analysis", *Earthq. Eng. Struct. Dyn.*, **29**, 1-17.
- Fajfar, P. and Fischinger, M. (1987), "Non-linear seismic analysis of RC buildings: Implications of a case study", *European Earthq. Eng.*, **1**, 31-43.
- Giberson, A. (1969), "Two nonlinear beams with definitions of ductility", *J. Struct. Div.*, ASCE, **95**, 137-157.
- Hasgür, Z. (1997), "Intensity investigations of strong motion earthquakes at Italy, Yugoslavia, Anatolia and Armenia earthquake belt", *Proc. of the Symposium on the Behalf of Prof. Rifat Yarar*, TDV/KT 97-003, **1**, Istanbul, December.
- Hasgür, Z., Taskin, B. and Nur, C. (2003), "Evaluation of the propriety of the non-linear analyses results with seismic damage indicators for R-C building structures", *Proc. of the Fifth National Conf. on Earthquake Engineering*, Istanbul, 26-30 May.
- Hoedajanto, D. (1983), "A model to simulate lateral force response of RC structures with cylindrical and box sections", Ph.D. Thesis, University of Llinois, Urbana Champaign, USA.
- Jennings, P.C., Housner, G.W. and Tsai, N.C. (1968), "Simulated earthquake motions", Report of Earthquake Engineering Research Laboratory, EERL-02, California Institute of Technology, USA.
- Johnson, E.A., Woitkiewicz, S.F. and Bergman, L.A. (1995), "Some experiments with massively parallel computation for M.C. simulation of stochastic dynamical systems", In: *Computational Stochastic Dynamics*, Spanos P.D. Editor, Balkema, Rotterdam, Netherlands, 325-336.
- Kabeyasava, T., Shiohara, H., Otani, S. and Aoyama, H. (1983), "Analysis of the full-scale seven Story R-C test structure", *J. of Faculty of Engrg.*, University of Tokio, **XXXVII**, 431-478.
- Kloeden, E.P. and Platen, E. (1992), *The Numerical Solutions of Stochastic Differential Equations*, Springer, Berlin.
- Kristensen, N.B. and Nørgaard, K. (1992), "Stokastisk responsanalyse af plastik deformerede dynamisk påvirkede 3D betonrammer", M. Sc. Thesis, University of Aalborg, Denmark.
- Lestuzzi, P. and Badoux, M. (2003), "The gamma-model: A simple hysteretic model for reinforced concrete walls", *Proc. of the Concrete Structures in Seismic Regions: FIB 2003 Symposium*, Athens, May.
- Lopez, R.R. (1988), "A numerical model for non-linear response of R/C frame-wall structures", Ph.D. Thesis, University of Llinois, Urbana Champaign, USA.
- Ma, S.M., Bertero, V.V. and Popov, E.P. (1976), "Experimental and analytical studies on the hysteretic behavior of RC rectangular and T-beams", Report of EERC, EERC-76-02, University of California, Berkeley, California.
- Midorikawa, M. and Kitagawa, Y. (1984), "U.S.-Japan cooperative research on R/C full-scale building test, Part 4: Dynamic characteristics of the building", *Proc. of the 8th World Conf. on EQ Eng.*, **VI**, USA, July 21-28, 619-625.
- Mochizuki, T. and Goto, N. (1983), "Structural system of buildings in Turkey and empirical evaluation of their seismic strength", *Comprehensive Study on Earthquake Disasters in Turkey in View of Seismic Risk Reduction*, Edited by: Ohta, Y., Sapporo, Japan.
- Mørk, K.J. (1989), "Stochastic response and reliability analysis of hysteretic structures", Ph.D. Thesis, University of Aalborg, Denmark.
- Mørk, K.J. and Nielsen, S.R.K. (1991), "System reduction of random dynamically loaded elasto-plastic structures", *Proc. of the Scandinavian Forum for Stochastic Mechanics*, Sweden, April.
- Mørk, K.J. (1992), "Stochastic analysis of reinforced concrete frames under seismic excitation", *Soil Dyn. Earthq. Eng.*, **11**, 145-161.
- Nielsen, S.R.K., Mørk, K.J. and Toft-Christensen, P. (1989), "Response analysis of hysteretic multi-story frames under earthquake excitation", *Earthq. Eng. Struct. Dyn.*, **18**, 655-666.

- OpenSees (2004), *Open System for Earthquake Engineering Simulation*, Pacific Earthquake Engineering Research Center, web site: <http://opensees.berkeley.edu/index.html>
- Otani, S. and Sözen, M. (1972), "Behavior of multistory reinforced concrete frames during earthquakes", Structural Research Series-392, University of Illinois-Urbana Champaign, IL.
- Otani, S. (1974), "SAKE: A computer program for inelastic response of RC frames subject to earthquakes", Civil Engineering Studies Technical Report-SRS-413, University of Illinois, Urbana.
- Pradlwarter, H.J. and Schuëller, G.I. (1999), "Assessment of low probability events of dynamical systems by controlled Monte Carlo simulation", *Probabilistic Engineering Mechanics*, **14**, 213-227.
- Prakash, V., Powell, G.H. and Campbell, S.A. (1993), "DRAIN-2DX: Base program description & user guide: Version 1.10", SEMM Report UCB/SEMM-1993/17, University of California, Berkeley, CA.
- Prakash, V., Powell, G.H. and Campbell, S.A. (1994), "DRAIN-3DX: Base program description & user guide", SEMM Report UCB/SEMM-1994/07, University of California, Berkeley, CA.
- Przemieniecki, J.S. (1968), *Theory of Matrix Structural Analysis*, McGraw-Hill Book Company, NY.
- Rodriguez-Gomez, S., Chung, Y.S. and Meyer, C. (1990), "SARCF-II User's guide: Seismic analysis of reinforced concrete frames", Technical Report NCEER-90-0027, State University of New York, Buffalo.
- Roufaiel, M.S.L. and Meyer, C. (1987), "Analytical modeling of hysteretic behavior of R/C frames", *J. Struct. Eng.*, ASCE, **113**, 429-444.
- Saatçioğlu, M. and Özcebe, G. (1989), "Response of reinforced concrete columns to simulated seismic loading", *ACI Struct. J.*, **86**, 3-12.
- Schuëller, G.I., Pradlwarter, H.J. and Schenk, C.A. (2003), "Nonstationary response of large linear FE models under stochastic loading", *Comput. Struct.*, **81**, 937-947.
- Shinozuka, M., Wen, Y.K. and Casciati, F. (1990), "Seismic damage and damage-control design for RC frames", *J. of Intelligent Material Systems and Structures*, **1**, 476-495.
- Sobczyk, K. and Trębicki, J. (2000), "Stochastic dynamics with fatigue-induced stiffness degradation", *Probabilistic Engineering Mechanics*, **15**(1), 91-99.
- Spencer, B.F.J. and Bergman, L.A. (1993), "On the numerical solution of the Fokker-Planck equation for nonlinear stochastic systems", *Nonlinear Dynamics*, **4**, 357-372.
- Takeda, T., Sözen, M.A. and Nielsen, N.N. (1970), "Reinforced concrete response to simulated earthquakes", *J. the Struct. Div.*, ASCE, **96**(ST12), 2557-2573.
- Taskin, B. (2001), "Non-linear stochastic analysis of 3D reinforced-concrete shear wall-frame structures under seismic excitation", Ph.D. Thesis, Istanbul Technical University, Turkey.
- Taskin, B. and Hasgür, Z. (2003), "Determining the non-linear behavior of 3D, R-C shear wall-frame structures with a stochastic approach", *ARI-Bulletin of the Istanbul Technical University*, **53**(1), 102-109.
- Turkish Earthquake Resistant Design Code, (1997), Ministry of Settlement and Public Works, Ankara, Turkey.
- Umemura, H., Iyoshi, M., Matsuzawa, A. and Ichinose, T. (2001), "Modeling of hysteresis rule of reinforced concrete structure considering strength degradation due to cyclic loading", *Proc. of the Eighth East Asia-Pacific Conf. on Structural Engineering and Construction: Challenges in the 21st Century: EASEC-8*, Nanyang Technological University, Singapore, September.
- Valles, R.E., Reinhorn, A.M., Kunnath, S.K., Li, C. and Madan, A. (1996), "IDARC 2D Version 4.0: A program for the inelastic damage analysis of buildings", Technical Report NCEER-96-0010, State University of New York, Buffalo.
- Wen, Y.K. (1989), "Methods of random vibration for inelastic structures", *Appl. Mech. Rev.*, **42**(2), 42-52.